

# Electronic Structure and Magnetism of Equiatomic FeN

Y. Kong

*Department of Physics & The Applied Magnetism Laboratory of the Ministry  
of Education, Lanzhou University, 730000 Lanzhou, China  
Max-Planck-Institut für Festkörperforschung, Heisenbergstr. 1, D-70569 Stuttgart, Germany*

## Abstract

In order to investigate the phase stability of equiatomic FeN compounds and the structure-dependent magnetic properties, the electronic structure and total energy of FeN with NaCl, ZnS and CsCl structures and various magnetic configurations are calculated using the first-principle TB-LMTO-ASA method. Among all the FeN phases considered, the antiferromagnetic (AFM) NaCl structure with  $q = (0, 0, \pi)$  is found to have the lowest energy at the theoretical equilibrium volume. However, the ferromagnetic (FM) NaCl phase lies only 1mRy higher. The estimated equilibrium lattice constant  $a^{th}=4.36\text{\AA}$  for nonmagnetic (NM) ZnS-type FeN agrees quite well with the experimental value of  $a^{exp}=4.33\text{\AA}$  but for AFM NaCl phase the  $a^{th}=4.20\text{\AA}$  is 6.7% smaller than the value observed experimentally. For ZnS-type FeN, metastable magnetic states are found for volumes larger than the equilibrium value. With the analysis of atom- and orbital-projected density of states (DOS) and orbital-resolved crystal orbital Hamilton population (COHP) the iron-nitrogen interactions in NM-ZnS, AFM-NaCl and FM-CsCl structures are discussed. The leading Fe-N interaction is due to the  $d$ - $p$  iron-nitrogen hybridization while considerable  $s$ - $p$  and  $p$ - $p$  hybridizations are also observed in all three phases. The iron magnetic moment  $\mu_{Fe}$  in FeN is found to be highly sensitive to the nearest-neighboring Fe-N distance. In particular, the  $\mu_{Fe}$  in ZnS and CsCl structures show an abrupt drop from the value of about  $2\mu_B$  to zero with the reduction of the Fe-N distance.

**Keywords:** FeN, TB-LMTO-ASA, magnetism, electronic structure

# 1 Introduction

For a long time iron nitride has attracted much scientific interest in basic research as well as in technology-oriented research. While a large number of results for iron-rich nitrides, such as  $\gamma'$ -Fe<sub>4</sub>N, have appeared in the literature[1], only a few investigations on high N-content FeN, specifically FeN[2, 3] with the proportionality 1:1 of Fe and N atoms were reported. Recently, two kinds of FeN structures have been determined in FeN films[4, 5, 6] synthesized by sputtering technique. They are the sodium chloride structure with lattice constants  $a=4.5\text{\AA}$  and the zinc blende structure with lattice constant  $a\approx 4.33\text{\AA}$ . All the prepared FeN films were non-stoichiometric due to N vacancies and/or impurities. <sup>57</sup>Fe Mössbauer spectroscopy experiments[4, 7] have shown that at 4.2K no magnetic hyperfine splitting is observed for ZnS-type FeN, but two kinds of Fe sites in NaCl-type FeN exhibit surprisingly large hyperfine fields of 49T and 30T. It was suggested that the ZnS-type FeN is nonmagnetic (NM) while the NaCl-type FeN shows antiferromagnetic (AFM) coupling[4, 7]. However, the magnetic measurements by Suzuki *et al.*[5] indicated that at low temperature the stoichiometric ZnS-type FeN is AFM and exhibits a micromagnetic character.

Using a full-potential linearized-augmented-plane-wave (FLAPW) method, Shimizu *et al.*[8, 9] calculated the electronic, structural and magnetic properties of stoichiometric ZnS- and NaCl-type FeN and estimated the equilibrium lattice constants and bulk moduli. The results indicated that the ferromagnetic (FM) NaCl-type FeN was more stable than the NM-ZnS structure. Furthermore, the calculated results[9] for the NaCl-type FeN with NM, FM,  $(\pi, \pi, \pi)$ - and  $(0, 0, \pi)$ -AFM configurations identified that the FM structure was the ground state with equilibrium lattice constant  $a^{th} \sim 4.0\text{\AA}$ . It has further shown that at the experimental lattice constant  $4.5\text{\AA}$  the  $(\pi, \pi, \pi)$ -AFM state was more stable than the FM state. A similar detailed analysis was not carried out for the ZnS-type FeN and the reason for the difference in magnetism between the two structures was therefore not clear. Most recently, Eck *et al.*[10] performed band structure calculations using tight-binding-linear-muffin-tin-orbitals (TB-LMTO) method within the atomic-sphere-approximation (ASA) and investigated structural and electronic properties of both FeN structures by analyzing density of states (DOS) and crystal orbital Hamilton population (COHP). They concluded that the zinc blende structure should be more stable because of the weaker antibonding Fe-Fe interactions below the Fermi level. Moreover, the authors evaluated the theoretical lattice constants for non-stoichiometric FeN and found that the deficiency of N atom decreases the equilibrium lattice constant. The magnetic properties of FeN were however hardly discussed. To achieve a better understanding of the magnetic diversity in FeN, systematic investigation

of the electronic structure and magnetic properties of various FeN structures thus seems to be needed.

In this paper, the TB-LMTO-ASA method is applied to calculate band structures of FeN compounds with various structures and spin configurations. The structural, electronic and magnetic properties of the FeN are thus investigated by analyzing the calculated electronic structure and total energy. In addition to the NaCl and ZnS structures, we also consider FeN in the CsCl structure.

A brief description of computational technique will be given in the next section. In section 3, we present the calculated total energy and electronic structural and discuss the structure and magnetic properties of FeN compounds. A short summary is given in the last section.

## 2 Computational Details

In the present study the electronic structures of equiatomic FeN compounds are calculated self-consistently using the scalar-relativistic TB-LMTO method[12] in the atomic-sphere-approximation including the combined correction. A local-density-approximation (LDA)[13] to the density-functional theory (DFT) is applied and the non-local correction is also included using the Perdew-Wang generalized-gradient-approximation (GGA).[14]

The lattice structures of NaCl-, ZnS- and CsCl-type FeN compounds are illustrated in Fig. 1. The Fe atoms in sodium chloride and zinc blende structures form an fcc lattice with different coordination of the N atoms. In the NaCl structure the N atoms are located at octahedral sites of the fcc lattice and each Fe atom has six N neighbors while in the ZnS structure the half-filling of the N atoms in tetrahedral sites of the fcc lattice makes each Fe four-fold coordinated to N atoms. In the cesium chloride structure the N atoms fill the body-centered sites of a simple-cubic Fe lattice and one Fe is eight-fold coordinated to N. The sites and filling fractions of the N atoms, the experimental magnetic structure, the nearest-neighbor (NN) Fe-Fe and Fe-N distances as well as the number of N neighbors of an Fe atom are summarized for the different structures in Table 1.

We perform NM, FM and  $(0, 0, \pi)$ -AFM calculations for FeN with NaCl, ZnS and CsCl structures. Besides  $(0, 0, \pi)$ -AFM state, the  $(\pi, \pi, \pi)$ -AFM configuration and an additional AFM structure[11], which consists of double layers with FM interlayer coupling along  $[001]$ -direction, AFMD, are also considered for NaCl-type FeN to include possible magnetic coupling in FeN film. The  $k$ -space integration is performed with the tetrahedron method[15] using  $16 \times 16 \times 16$  mesh within the Brillouin zone. All partial waves with  $l \leq 2$  are included in the basis for Fe as well as N. For ZnS- and NaCl-type FeN, special care is taken in filling

the interatomic space since the structures are rather open. Therefore, it is necessary to introduce interstitial spheres. The sphere radii and the positions of interstitial spheres are chosen in such a way that space filling is achieved without exceeding a sphere overlap of 16%. This is done using an automatic procedure developed by Krier *et al.*[16]. The radii of atomic and interstitial spheres corresponding to the theoretical equilibrium volume are listed in Table 2 for the different FeN structures.

In combination with the analysis of atom- and orbital-projected density of states (DOS), the COHP technique[17] is applied to analyze the chemical bonding in ZnS-, NaCl- and CsCl-type FeN to examine the different Fe-N interactions. This technique provides information analogous to the Crystal Orbital Overlap Population (COOP) analysis.[18] While COOP curves are energy resolved plots of the Mulliken overlap population between two atoms or orbitals, a COHP curve is an energy resolved plot of the contribution of a given bond to the bonding energy of the system. Similar to COOP curves, in all the COHP curves presented here positive values are bonding and negative antibonding, i.e.  $-\text{COHP}$  is plotted instead of COHP.

### 3 Results and Discussions

#### 3.1 Total energy and phase stability

The calculated total-energy curves for ZnS-, NaCl- and CsCl-type FeN with NM, FM and AFM spin configurations are shown in Fig. 2. The theoretical equilibrium lattice constants  $a^{th}$  are estimated for various FeN phases and they are listed in Table 2 together with total energies at  $a^{th}$ . The total-energy for NM CsCl structure is not plotted in Fig. 2 because the values are much higher than the other phases.

Firstly, we shall discuss the total-energy curves for NaCl-type FeN. Except for the NM NaCl-type FeN with higher energy, the magnetic NaCl phases with different spin configurations give similar total-energy curves. As indicated in Table 2, at the equilibrium volume the  $E^{th}$  for  $(0, 0, \pi)$ -AFM phase is only 1mRy lower than that for FM-NaCl structure and 10mRy below the highest  $(\pi, \pi, \pi)$ -AFM structure. Although our results are in better agreement with experiment than previous results[9], the  $a^{th}$  ( $\sim 4.20\text{\AA}$ ) estimated for NaCl-type FeN is still 6.7% smaller than the values observed experimentally. This discrepancy is much larger than the normal deviation due to the local density approximation (LDA) with GGA correction. It may therefore be, as suggested in Refs.[9, 10], that the experimental NaCl-type FeN with  $a=4.5\text{\AA}$  is not in stable state due to unknown effects, such as the effect of the surface.

We also perform total-energy calculations for magnetic NaCl phases without the inclusion

of the GGA correction to the LDA. The estimated theoretical lattice constants for magnetic NaCl phases are about  $3.96\sim 4.01\text{\AA}$ , which are smaller than those obtained with GGA, and the FM phase is found to be stable at the theoretical equilibrium volume. The results are consistent with those by Shimizu *et al.*[9]. In the following only the results calculated with the GGA correction are presented.

For ZnS-type FeN, a NM ground state is found with theoretical equilibrium lattice constant  $a^{th}=4.36\text{\AA}$ , which agrees quite well with the experimental value[4]. The state is about 6mRy higher in energy than that of the  $(0,0,\pi)$ -AFM NaCl structure. Self-consistent  $(0,0,\pi)$ -AFM and FM solutions are found when the lattice constant is larger than  $4.45\text{\AA}$  and  $4.69\text{\AA}$ , respectively. Since the critical lattice constant  $4.45\text{\AA}$  for the  $(0,0,\pi)$ -AFM state is only  $0.09\text{\AA}$  larger than  $a^{th}$  of the NM-ZnS phase, one could expect that the metastable AFM phase would be important for the observed micromagnetic character in ZnS-type FeN.[5]

The total-energy curves calculated for FM and  $(0,0,\pi)$ -AFM CsCl-type FeN are nearly identical and about 70mRy above those of ZnS and NaCl structures. Because of this rather higher total-energy, the CsCl-structure should not be considered a possible stable FeN phase.

Among all the investigated FeN phases, as mentioned above, the simple  $(0,0,\pi)$ -AFM NaCl structure is found to have the lowest total energy at theoretical equilibrium volume, while the  $E^{th}$  for FM-NaCl structure is only about 1mRy higher. However, the energy difference is very small and may be of the order of the inaccuracies due to the ASA used in our calculations.

### 3.2 Electronic structure and iron-nitrogen interactions

In the following, the electronic structure and Fe-N interactions in the FeN phases will be analyzed in detail using the calculated DOS and COHP for NM ZnS,  $(0,0,\pi)$ -AFM NaCl and FM CsCl structures. In Fig. 3 we show the spin-resolved DOS for NM ZnS-,  $(0,0,\pi)$ -AFM NaCl- and FM CsCl-type FeN at the theoretical equilibrium volume. The DOS at Fermi level,  $N(E_F)$ , are listed in Table 2.

Except for the  $s$ -like states around  $-15\text{eV}$ , which are not shown, the DOS of NM-ZnS structure shown in Fig. 3a mainly consists of two sets of structures, which are separated by a 2eV energy gap. The lower energy set, centered around  $-6\text{eV}$ , is primarily composed of N  $2p$  bands with some admixture of Fe  $d$ -character, the higher energy set from  $-2.3$  to  $3.6\text{eV}$ , is dominated by Fe  $3d$  states. A small gap at  $-0.5\text{eV}$  further divides the latter into two parts, which are respectively characterized by the crystal-field splitted  $e$  and  $t_2$  sets. The Fermi-level  $E_F$  is located just above the gap at the low-energy side of the  $t_2$  set. The reason for ZnS-type FeN phase showing no magnetic moment at equilibrium volume may be

understood from the DOS at the  $E_F$ . According to the Stoner model the self-consistency condition for a ferromagnet can be simply expressed by

$$N(E_F) \cdot I = 1$$

where  $N(E_F)$  is the paramagnetic density of state at the  $E_F$  and  $I$  the effective Stoner interaction parameter. For the ZnS-type FeN, it is observed that the DOS curve intersects the Fermi-level with a large negative slope and gives a quite small  $N(E_F)$  (0.7 states/eV·spin). Consequently, no magnetic ordering is observed for ZnS-type FeN. On the other hand, by increasing the volume, the 3d subband becomes much narrower and the  $N(E_F)$  larger. The Stoner criterion may therefore be satisfied and the ZnS-type FeN shows certain magnetic ordering. Indeed, our total-energy calculations for ZnS-type FeN has confirmed the metastable FM and AFM phases existing at larger volumes.

Since the band structures of two sublattice in AFM phase are identical, in Fig. 3b only the sublattice DOS for (0,0, $\pi$ )-AFM NaCl structure is plotted. Compared to that of NM ZnS phase, the DOS of (0,0, $\pi$ )-AFM NaCl-type FeN form a continuous spectrum over the energy range between  $-8$  and  $4$  eV. Due to the large dispersion of Fe 3d subbands the expected crystal field splitting of 3d orbitals can not be clearly seen. While the majority-spin DOS are nearly completely occupied, a dominant minority-spin peak is located above the Fermi level due to the exchange-splitting. In Fig. 3c the peaks of the DOS for FM CsCl structure also show complicated structure. Compared to that of NaCl structure, the DOS of the CsCl-type FeN exhibits larger dispersion. Below the  $E_F$ , the majority-spin DOS peaks of NaCl and CsCl structures have a tendency to split into two parts by a deep valley at about  $-3$  and  $-4$  eV, respectively. The higher part is dominated by Fe 3d states while the lower one is mostly composed of N 2p with some admixture of Fe d states.

The partial DOS (PDOS) of FeN with NM ZnS, (0,0, $\pi$ )-AFM NaCl and FM CsCl structures, projected for Fe  $s$ ,  $p$ ,  $d$  and N  $p$  orbitals, are plotted in Fig. 4. Correspondingly, Fig. 5 shows the orbital-projected COHP calculated for the  $s$ - $p$ ,  $p$ - $p$  and  $d$ - $p$  iron-nitrogen interactions. Here only the nearest-neighbor contributions are included in the COHP. Noticed that of the two identical sublattices in (0,0, $\pi$ )-AFM-NaCl phase, only the PDOS for one sublattice are shown in Fig. 4b while the COHP curves for Fe<sub>1</sub>-N<sub>1</sub> (Fe<sub>2</sub>-N<sub>2</sub>) intra-sublattice and Fe<sub>1</sub>-N<sub>2</sub> (Fe<sub>2</sub>-N<sub>1</sub>) inter-sublattice interactions are presented in Fig. 5b and 5c, respectively. Here Fe<sub>1</sub> (N<sub>1</sub>) defines the Fe (N) atom in the up-polarized sublattice and Fe<sub>2</sub> (N<sub>2</sub>) the atom in the down-polarized sublattice.

Consistent with the observation of the total DOS, a 2eV energy gap separates the PDOS of NM ZnS phase, shown in Fig. 4a, into two sets of isolated structures. As indicated by the COHP curves in Fig. 5a, N  $p$  orbitals mix Fe  $s$ ,  $p$  and  $d$  subbands on both side of

the gap but the  $d$ - $p$  hybridization dominates the iron-nitrogen interactions. The  $d$ - $p$  Fe-N hybridization is characterized by the large bonding peaks below the gap, centered at about  $-5\text{eV}$ , and the antibonding peaks around the Fermi-level, centered at about  $2.0\text{eV}$ . On the contrary, in both energy windows the  $s$ - $p$  and  $p$ - $p$  hybridizations form bonding interactions. The corresponding antibonding interactions lie far above the Fermi-level.

In  $(0,0,\pi)$ -AFM NaCl structure, the PDOS projected for Fe  $s, p, d$  and N  $p$  orbitals (Fig. 4b) spread over the same energy range from  $-8$  to  $4.0\text{eV}$  without energy gap and show prominent hybridizations in the entire energy range. According to the calculated COHP shown in Fig. 5b and Fig. 5c, the  $d$ - $p$  hybridization in NaCl-type FeN is characteristic of the bonding interactions below  $-3\text{eV}$  and the antibonding states above  $-3\text{eV}$ . Furthermore, it is found that the antibonding peaks below the  $E_F$  are dominated by antibonding  $\pi^*$  states and the peaks above the  $E_F$  are mainly  $\sigma^*$  states in character. Comparing the  $d$ - $p$  interactions in Fig. 5b and Fig. 5c, a stronger antibonding  $\pi^*$  peak at  $-2\text{eV}$  is observed for inter-sublattice Fe-N hybridization. Except for the leading  $d$ - $p$  interactions the  $s$ - $p$  and  $p$ - $p$  hybridization show considerable bonding interactions from  $-8$  to  $4\text{eV}$ . In contrast to the  $d$ - $p$  interaction, the  $s$ - $p$  and  $p$ - $p$  interactions for both intra- and inter-sublattice Fe-N interactions are nearly identical. Compared to the ZnS structure, the antibonding peaks of  $s$ - $p$  and  $p$ - $p$  hybridization in NaCl structure are shifted towards lower energy.

Due to larger Fe-N distance, the Fe-N interactions in FM CsCl structure is much weaker than that in ZnS and NaCl structure. As also observed in  $(0,0,\pi)$ -AFM NaCl structure, the dominant Fe-N  $d$ - $p$  hybridization is composed of the bonding set at lower energy and the antibonding set around the  $E_F$ . Below the  $E_F$  there exist strong antibonding peaks. For  $s$ - $p$  and  $p$ - $p$  interactions the antibonding peaks are found to be much lower in energy than those in ZnS and NaCl structures.

Although the  $s$ - $p$  and  $p$ - $p$  hybridizations give inevitable contributions, as indicated by the COHP curves in Fig. 5, the dominant Fe-N interaction in all the three FeN structures is the  $d$ - $p$  hybridization. In Fig. 5 we also plot the integrated COHP for  $d$ - $p$  interactions. As indicated by the ICOHP at Fermi level, the ZnS-type FeN exhibits the strongest  $d$ - $p$  Fe-N hybridization among the three FeN structures because of the shortest nearest-neighboring Fe-N distance. On the contrary, the largest Fe-N distance in CsCl structure makes the CsCl-type FeN showing the weakest Fe-N hybridization although the Fe atoms in this structure has the most N neighbors.

### 3.3 Magnetic moment and its volume dependence

The calculated iron magnetic moments  $\mu_{Fe}$  for the different FeN phases at the theoretical equilibrium volume are listed in table 2. For all the four magnetic NaCl-type FeN phases a similar value of  $\mu_{Fe}$  is obtained. Among them the FM phase produces a slightly larger  $\mu_{Fe}$ . For both FM and AFM CsCl-type FeN the calculated Fe magnetic moments are larger than those in NaCl-type FeN. At equilibrium volume no spin-splitting for FeN with ZnS structure is obtained from spin-polarized FM and AFM calculations. Noticed that the Fe-N interaction in ZnS structure is the strongest and that in CsCl structure the weakest, it is reasonably concluded that the magnetic properties of Fe in FeN structures is strongly correlated to the strength of the Fe-N interactions, mainly  $d-p$  hybridization. In other words, the magnetic properties of FeN phases is closely related to the nearest-neighboring Fe-N distance in the structure. The stronger the Fe-N hybridization is, the smaller becomes the Fe magnetic moment.

The Fe magnetic moments in magnetic NaCl-, CsCl- and ZnS-type FeN calculated at various volumes are shown in Fig. 6 as a function of the nearest-neighboring Fe-N distance,  $d_{Fe-N}$ . It is found that the  $\mu_{Fe}$  is highly sensitive to the  $d_{Fe-N}$ . By compressing the volume, the Fe magnetic moment in all the magnetic FeN phases dramatically decrease with the reduction of the  $d_{Fe-N}$ . While  $\mu_{Fe}$  in NaCl-type FeN decrease with  $d_{Fe-N}$  at nearly the same rate and it becomes zero gradually when the  $d_{Fe-N}$  is smaller than about  $3.3\text{\AA}$ ,  $\mu_{Fe}$  in both CsCl and ZnS structures exhibit a sudden drop from a value of about  $2\mu_B$  to zero at a certain critical  $d_{Fe-N}$ . According to the canonical band model[19], the different volume dependence of the  $\mu_{Fe}$  in various FeN structures should be related to the difference of the DOS around the  $E_F$ .

## 4 Conclusions

Starting out from the calculated total energy and electronic structure using the TB-LMTO-ASA method, we have investigated structural, electronic and magnetic properties of FeN compounds with NaCl, ZnS and CsCl structures.

From the calculated total-energy a stable  $(0,0,\pi)$ -AFM NaCl-type FeN with theoretical equilibrium lattice constant  $a = 4.2\text{\AA}$  is identified. For the FeN with ZnS structure, our results indicate the existence of metastable AFM and FM solutions with a larger cell volume besides stable NM phase. These metastable states may be important for the observed micromagnetic character in ZnS-type FeN.

By analyzing the atom- and orbital-resolved density of states and the orbital-projected



COHP, the Fe-N hybridization interactions in NM ZnS,  $(0,0,\pi)$ -AFM NaCl and FM CsCl structures are discussed in detail. In all the three considered FeN structures the  $d$ - $p$  hybridization between Fe and N atoms dominates the Fe-N interactions. With the calculated Fe magnetic moment for various FeN structures, it is suggested that the magnetic properties of FeN phases are closely related to the strength of the Fe-N  $d$ - $p$  hybridization. Furthermore, the Fe magnetic moment in FeN phases are found to be highly sensitive to the nearest-neighboring Fe-N distance.

Finally, it should be mentioned that the equilibrium lattice constant  $a^{th}$  estimated for NaCl-type FeN is 6.7% smaller than the values observed experimentally though in our calculations the GGA correction to the local density approximation has been applied. It is suggested that other unknown effects should be responsible for the extraordinarily larger lattice constant observed for FeN with NaCl structure. Eck et al.[10] have estimated the equilibrium lattice constant for defected FeN and obtained a rather smaller  $a^{th}$ . Up to date, no theoretical investigations on FeN film has been reported. It is highly desired to perform calculations on FeN structure with low-dimensional symmetry so that the effect of surface may be examined.

## Acknowledgements

The author would like to gratefully acknowledge Prof. O.K. Andersen for many helpful advices and is indebted to Dr. O. Jepsen for a careful reading of the manuscript.

## References

- [1] P. Mohn and S.F. Matar, J. Magn. Magn. Mater., **191**, 234(1999), and the references listed therein.
- [2] N. Heiman and N.S. Kazama, J. Appl. Phys., **52**, 3562(1981).
- [3] A. Oueldennaoua, E. Bauer-Grosse, M. Foos and C. Frants, Scr. Metall., **19**, 1503(1985).
- [4] H. Nakagawa, S. Nasu, H. Fujii, M. Takahashi and F. Kanamaru, Hyper. Inter., **69**, 455(1991).
- [5] K. Suzuki, H. Morita, T. Kaneko, H. Yoshida and H. Fujimori, J. Alloys & Compounds, **201**, 11(1993).
- [6] L. Rissanen, M. Neubauer, K.P. Lieb, P. Schaaf, J. Alloys & Compounds, **274**, 74(1998).
- [7] T. Hinomura and S. Nasu, Hyper. Inter., **111**, 221(1998).
- [8] H. Shimizu, M. Shirai and N. Suzuki, J. Phys. Soc. Jap., **66**, 3147(1997).
- [9] H. Shimizu, M. Shirai and N. Suzuki, J. Phys. Soc. Jap., **67**, 922(1998).
- [10] B. Eck, R. Dronskowski, M. Takahashi and S. Kikkawa, J. Mater. Chem., **9**, 1527(1999).
- [11] H.C. Herper, E. Hoffmann and P. Entel, Phys. Rev. B **60**, 3839(1999).
- [12] O.K. Andersen and O. Jepsen, Phys. Rev. Lett. **53**, 2571(1984); G. Krier, O. Jepsen, A. Burkhardt and O.K. Andersen, The Stuttgart TB-LMTO-ASA program.
- [13] S.H. Vosko, L. Wilk and M. Nusair, Can. J. Phys., **58**, 1200(1980).
- [14] J.P. Perdew and Y. Wang, Phys. Rev. B **45**, 13244(1992).
- [15] O. Jepsen and O.K. Andersen, Solid State Commun. **9**, 1763(1971) and Phys. Rev. B **29**, 5965(1984); P. Blöchl, O. Jepsen and O.K. Andersen, Phys. Rev. B **49**, 16223(1994).
- [16] G. Krier, O.K. Andersen, O. Jepsen (unpublished).
- [17] R. Dronskowski and P.E. Blöchl, J. Phys. Chem., **97**, 8617(1993).
- [18] T. Hughbanks and R. Hoffmann, J. Am. Chem. Soc., **105**, 3528(1983).
- [19] O.K. Andersen, J. Madsen, U.K. Poulsen, O. Jepsen and J. Kollar, Physica, **86-88B**, 249(1977).

## Tables

Table 1: The site and filling fraction (per cubic cell) of the N atoms in FeN compounds, lattice constant  $a$  and magnetic structures.  $d_{Fe-Fe}$  and  $d_{Fe-N}$  are the nearest-neighbor Fe-Fe and Fe-N distances at the experimental lattice constant.  $n$  is the number of N neighbors of one Fe atom. Since the CsCl-type FeN does not exist, the calculated results are given.

Structure type	ZnS	NaCl	CsCl
Site	tetrahedral	octahedral	body-centered
filling fraction	4/8	4/4	1/1
exp. mag. structure	NM	AFM	FM
$a$ (Å)	4.33[4]	4.50[4]	2.63
$d_{Fe-Fe}$ (Å)	3.04	3.18	2.63
$d_{Fe-N}$ (Å)	1.86	2.25	2.28
$n$	4	6	8

Table 2: Calculated total energy, equilibrium lattice constant, DOS at  $E_F$  and Fe magnetic moment for some considered FeN structures.  $E^{th}$  is the total energy (given by E+2656.0 in Ry/FeN) at the theoretical equilibrium lattice constants  $a^{th}$ ,  $N(E_F)$  the DOS at Fermi level in states/eV·FeN and  $\mu_{Fe}$  the Fe magnetic moment at the  $a^{th}$ .  $S_{Fe}$  and  $S_N$  are the radii of Fe and N atomic spheres corresponding to the theoretical equilibrium volume and  $S_E$  the radius of interstitial sphere.

	ZnS	NaCl				CsCl	
	NM	(00 $\pi$ )-AFM	FM	AFMD	( $\pi\pi\pi$ )-AFM	FM	(00 $\pi$ )-AFM
$E^{th}$ (Ry)	-0.3844	-0.3901	-0.3892	-0.3856	-0.3799	-0.3148	-0.3147
$a^{th}$ (Å)	4.36	4.20	4.21	4.19	4.20	2.63	2.63
$S_{Fe}$ (Å)	1.166	1.329	1.332	1.326	1.329	1.425	1.425
$S_N$ (Å)	0.962	1.072	1.074	1.070	1.072	1.129	1.129
$S_E$ (Å)	1.166	0.750	0.752	0.749	0.750	-	-
	0.962	-	-	-	-	-	-
$\mu_{Fe}$ ( $\mu_B$ )	-	2.67	2.75	2.67	2.69	2.86	2.81
$N(E_F)$	1.40	1.90	2.42	2.39	1.03	1.57	1.98

## Figure Caption

Figure 1: Schematic illustration of FeN with NaCl (left), ZnS (middle) and CsCl (right) structures.

Figure 2: Calculated total energy vs. volume for FeN with ZnS, NaCl and CsCl structures. Here  $(0,0,\pi)$ -AFM and  $(\pi,\pi,\pi)$ -AFM denote phases showing antiferromagnetic coupling along  $[001]$ - and  $[111]$ -directions, respectively. AFMD is the AFM state which consists of double layers with FM interlayer coupling along  $[001]$ -direction. The arrows label the volume corresponding to experimental lattice constants of ZnS- and NaCl-type FeN.

Figure 3: Spin-resolved DOS calculated for FeN with (a) nonmagnetic ZnS, (b)  $(0,0,\pi)$ -AFM NaCl and (c) FM CsCl structures at the theoretical equilibrium volume. Solid lines represent the majority-spin DOS and dash lines the minority-spin DOS. The Fermi-level is at zero energy.

Figure 4: Orbital-projected partial DOS calculated for FeN with (a) NM ZnS, (b)  $(0,0,\pi)$ -AFM NaCl and (c) FM CsCl structures at theoretical equilibrium volume. The dash, dot, dash-dotted and solid lines represent the DOS projected for Fe  $s, p, d$  and N  $p$  orbitals. The Fermi-level is at zero energy.

Figure 5: The COHP curves calculated for  $s$ - $p$ ,  $p$ - $p$  and  $d$ - $p$  interactions between Fe and N atoms in FeN with (a) NM ZnS, (b) and (c)  $(0,0,\pi)$ -AFM NaCl and (d) FM CsCl structures. Here (b) and (c) show the Fe-N interactions within and between the sublattice in  $(0,0,\pi)$ -AFM NaCl structure, respectively. The solid, dash-dotted and dash lines represent  $s$ - $p$ ,  $p$ - $p$  and  $d$ - $p$  interactions. The integrated COHP (in eV/cell) for  $d$ - $p$  interaction are also plotted with thick solid lines.

Figure 6: Calculated Fe magnetic moment in FeN with ZnS, NaCl and CsCl structures as function of the nearest-neighboring Fe-N distance. The arrows indicate the distances corresponding to experimental lattice constants of NaCl- and ZnS-type FeN.

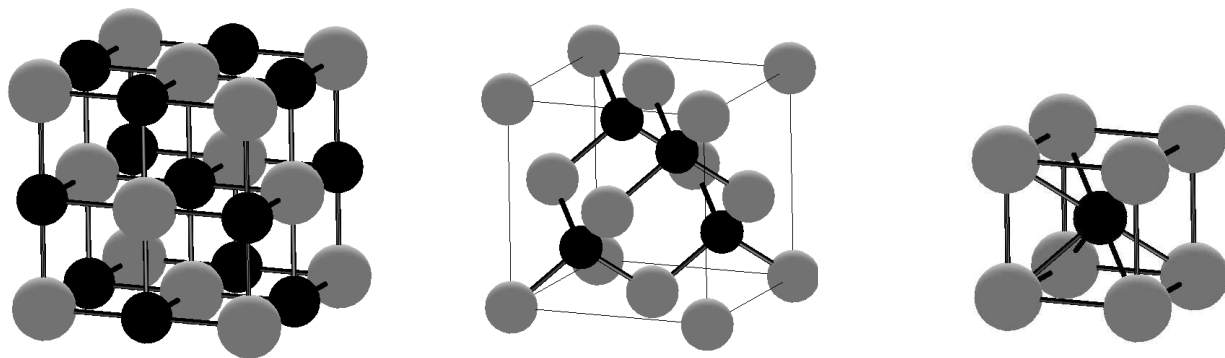


Fig. 1 of Y. Kong

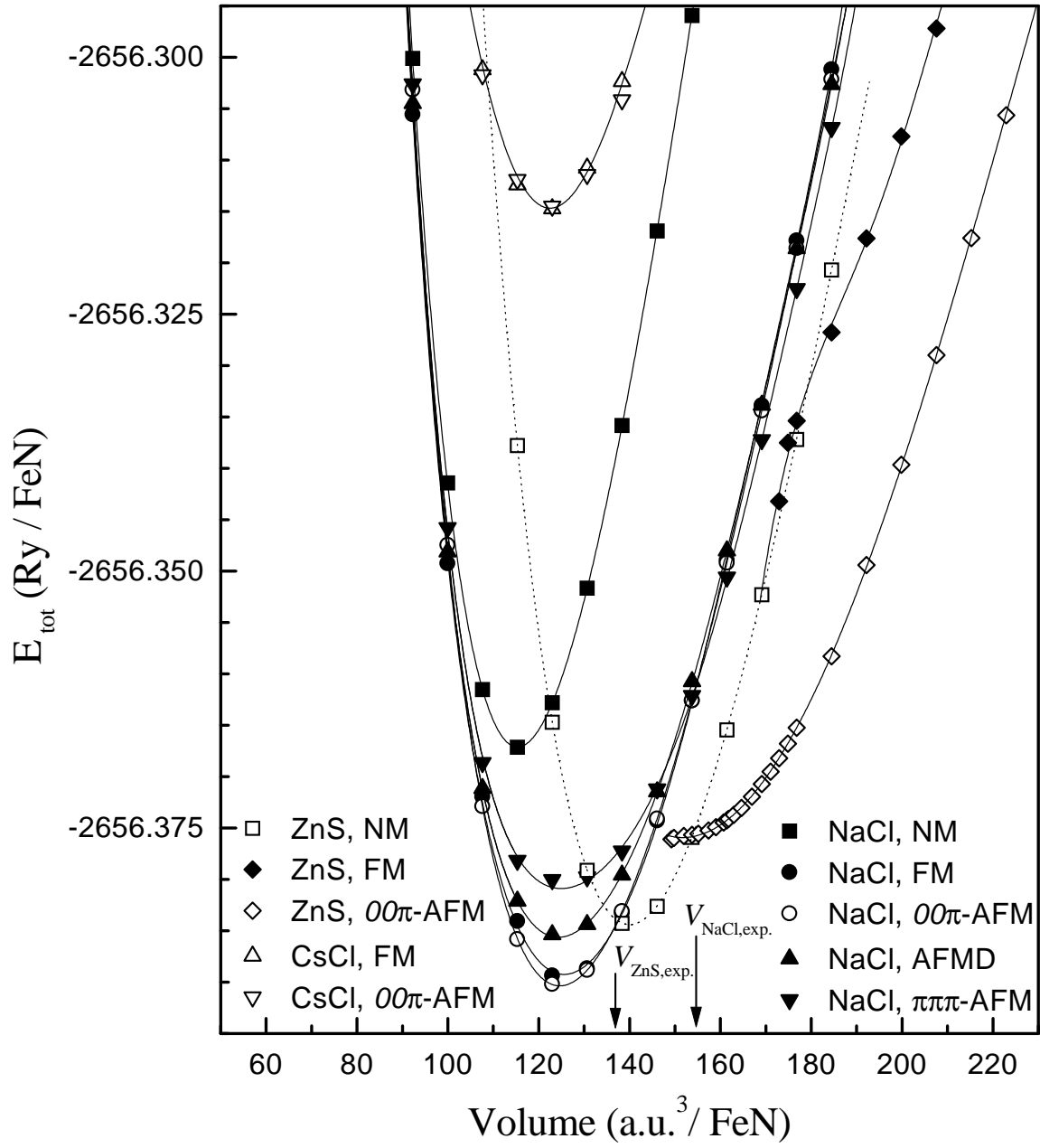


Fig. 2 of Y. Kong

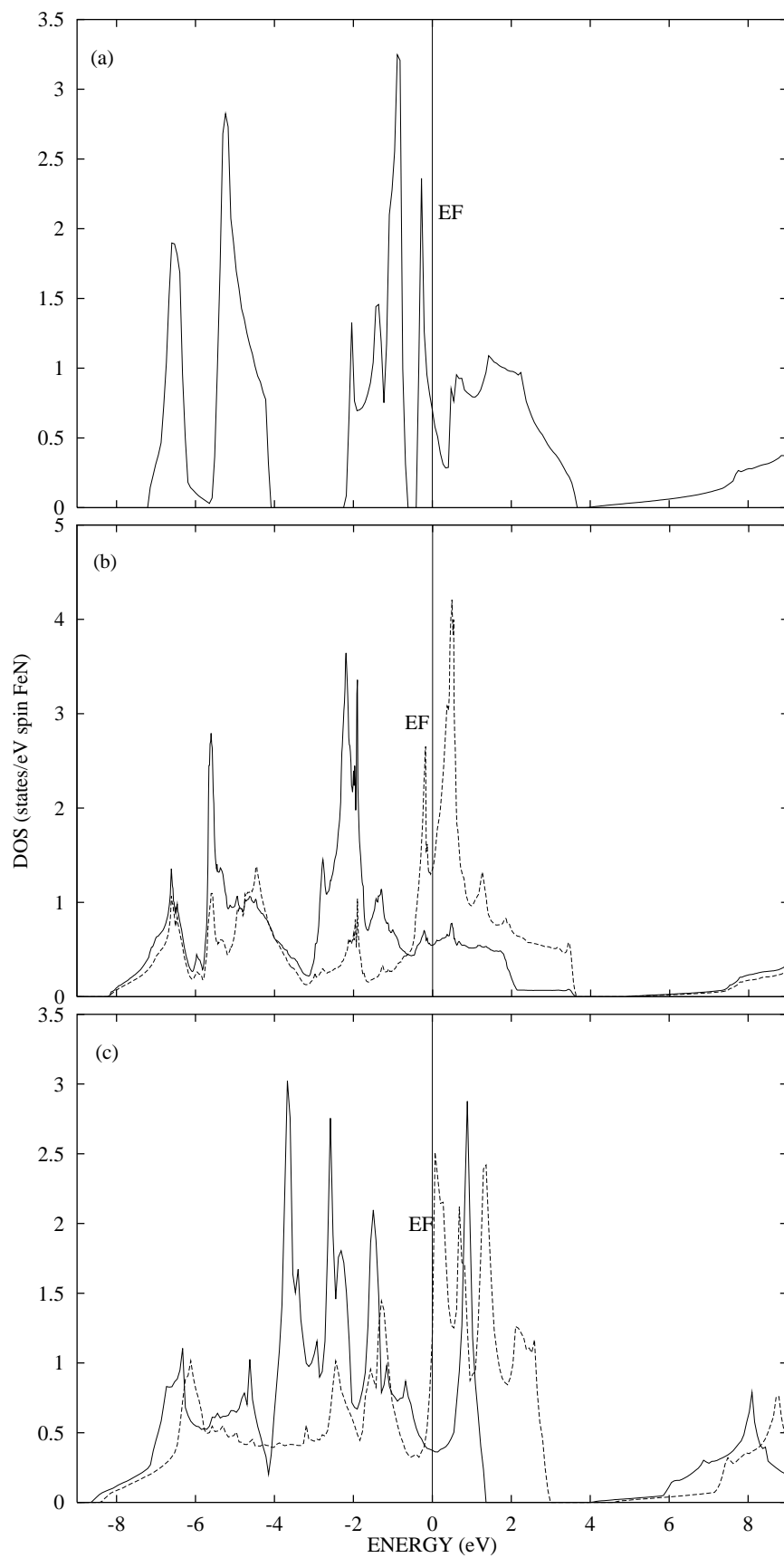


Fig. 3 of Y. Kong

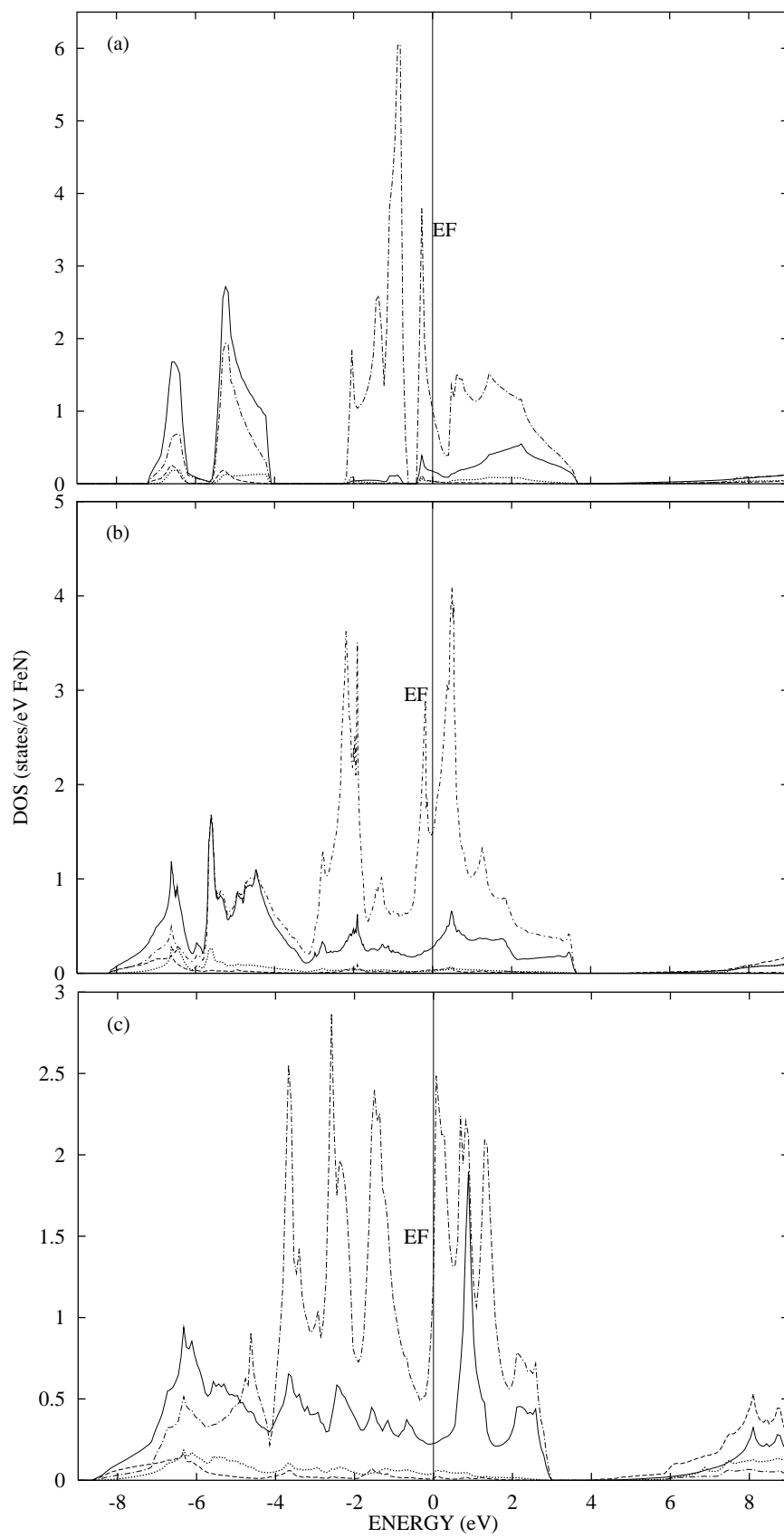


Fig. 4 of Y. Kong



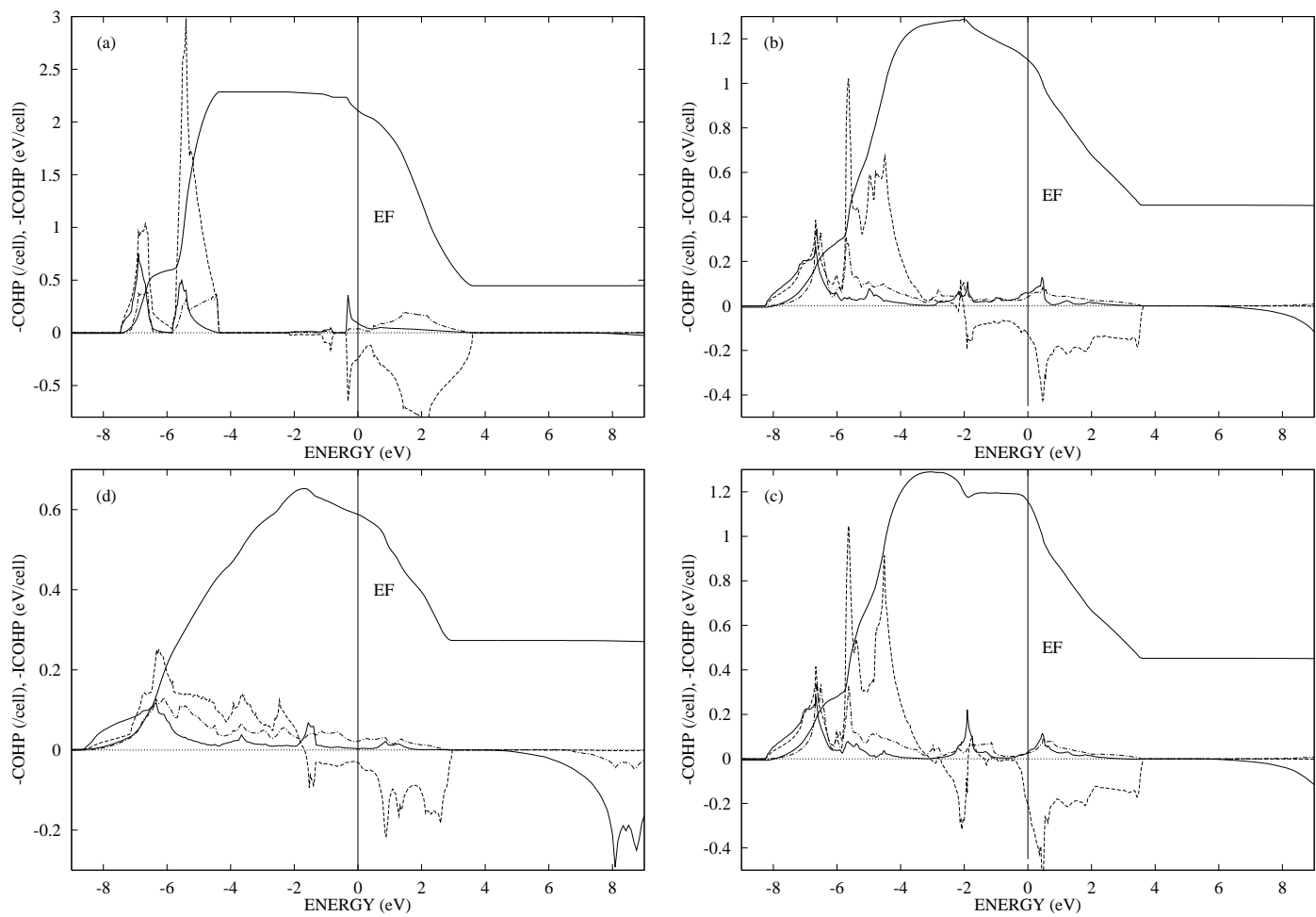


Fig. 5 of Y. Kong

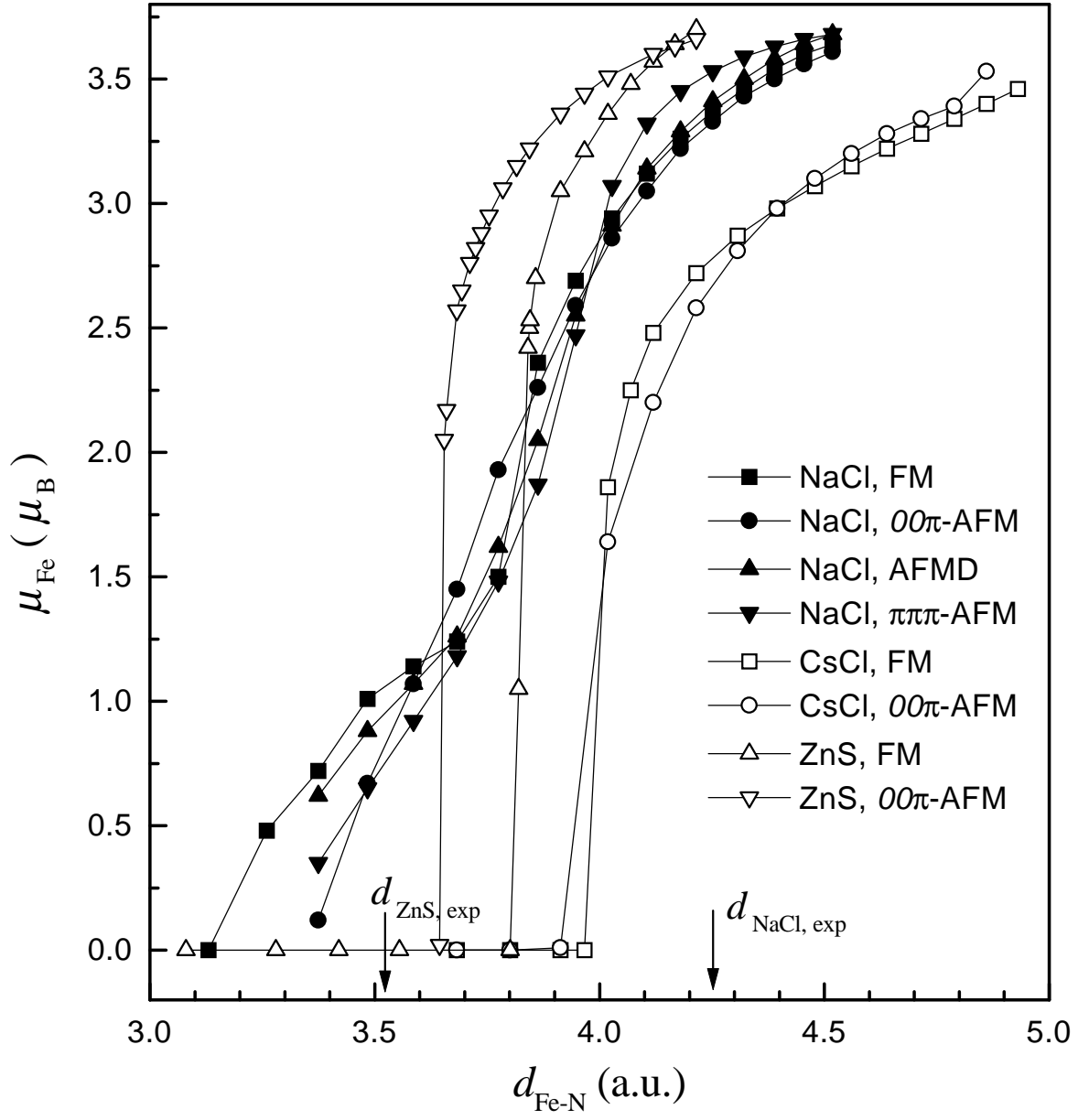


Fig. 6 of Y. Kong